Bone 127 (2019) 592–601

Contents lists available at ScienceDirect

Bone

journal homepage: www.elsevier.com/locate/bone

Full Length Article

Activation of G_q signaling by *Pasteurella multocida* toxin inhibits the osteoblastogenic-like actions of Activin A in C2C12 myoblasts, a cell model of fibrodysplasia ossificans progressiva

Julia K. Ebner[a,b,c], Gabriele M. König[d], Evi Kostenis[d], Peter Siegert[a], Klaus Aktories[a,c,e,*], Joachim H.C. Orth[a]

[a] Institute for Experimental and Clinical Pharmacology and Toxicology, Faculty of Medicine, University of Freiburg, Albertstr. 25, 79104 Freiburg, Germany
[b] Faculty of Biology, University of Freiburg, Schänzlestr. 1, 79104 Freiburg, Germany
[c] Spemann Graduate School for Biology and Medicine, University of Freiburg, Albertstr. 19A, 79104 Freiburg, Germany
[d] Molecular, Cellular and Pharmacobiology Section, Institute of Pharmaceutical Biology, University of Bonn, Nussallee 6, 53115 Bonn, Germany
[e] BIOSS Centre for Biological Signalling Studies, University of Freiburg, Schänzlestr. 18, 79104 Freiburg, Germany

ARTICLE INFO

Keywords:
Osteoblast differentiation
FOP
BMP
Activin A
Alk2
Smad

ABSTRACT

The human disease fibrodysplasia ossificans progressiva (FOP) is a rare and highly disabling disorder of extensive heterotopic bone growth that is caused by a point mutation (R206H) in the activation domain of Alk2, a BMP (bone morphogenic protein) type 1 receptor. The mutation leads to extensive BMP-signaling induced by Activin A, which is normally an antagonist for wildtype receptors, resulting in excessive and uncontrolled bone formation. Here, we studied the effects of *Pasteurella multocida* toxin (PMT), which activates osteoclasts and inhibits osteoblast activity, in C2C12 myoblasts expressing the mutant Alk2(R206H) receptor as model of FOP. In our study, we mainly used alkaline phosphatase (ALP) activity as marker to determine osteoblast differentiation.

BMP-4 stimulated an increase in ALP activity in C2C12-Alk2wt and C2C12-Alk2(R206H) cells. By contrast, Activin A only induced ALP activity in C2C12-Alk2(R206H) cells. In both cases, PMT acted as a potent inhibitor of ALP activity. PMT-induced inhibition of ALP activity was paralleled by a constitutive activation of the heterotrimeric G_q protein. Expression of a permanently active $G\alpha_q$ blocked Activin A/Alk2(R206H)-dependent increase in ALP activity. Inactivation of G_q by specific inhibitor FR900359 blocked the PMT effect. Similarly, canonical second messengers and effectors of $G\alpha_q$ (e.g. ionophore A23187-induced increase in intracellular Ca^{2+} and activation of PKC by PMA (phorbol 12-myristate 13-acetate)) inhibited Alk2(R206H)-mediated induction of ALP activity. Notably, Activin A-induced increase in ALP activity in C2C12-Alk2(R206H) cells was also inhibited by stimulation of the α_{1A}-adrenoceptor, which couples to $G\alpha_q$, by phenylephrine. PMT did not alter tail phosphorylation of the major downstream effectors of the Alk2 receptor, Smad1/5/9; neither did the toxin affect nuclear translocation of the Smad-complex. However, PMT diminished BMP responsive element-induced gene expression.

The data indicate that PMT potently inhibits the induction of osteoblast markers in a FOP model via activation of G proteins. Moreover, our findings indicate that activation of G protein-coupled receptors and of G protein signaling might be a rationale for pharmacological therapy of FOP.

1. Introduction

Fibrodysplasia ossificans progressiva (FOP) is a rare and highly disabling autosomal dominant disorder with symptoms of congenital skeletal malformations and progressive heterotopic ossification. In its ultimate stages, FOP causes immobility due to metamorphosis of skeletal muscle and soft tissue into a second skeleton [1,2]. Patients suffer from painful inflammatory flare-ups (soft tissue swellings) that transform soft connective tissue like fascia, ligaments, tendons and skeletal muscle into bones. Surgical removal of heterotopic bone causes

* Corresponding author at: Institute for Experimental and Clinical Pharmacology and Toxicology, Faculty of Medicine, University of Freiburg, Albertstr. 25, 79104 Freiburg, Germany.
E-mail address: klaus.aktories@pharmakol.uni-freiburg.de (K. Aktories).

https://doi.org/10.1016/j.bone.2019.07.031
Received 11 September 2018; Received in revised form 29 July 2019; Accepted 30 July 2019
Available online 31 July 2019
8756-3282/

episodes of rapid and painful new bone growth [2,3]. The majority of patients are bound to the wheelchair by their third decade of life and in their forties, most patients die from complications of the thoracic insufficiency syndrome [4].

Classical FOP patients show a single nucleotide exchange (c.617G > A) in the Acvr1/Alk2 gene resulting in a mutation (R206H) in the glycine-serine activation domain of bone-morphogenic-protein (BMP) Alk2 receptor [1]. This mutation activates the receptor by rendering Alk2(R206H) responsive to the normally inhibitory ligands such as Activin A [5,6]. Also, other mutations in the Acvr1 gene have been reported, leading to less drastic forms of FOP [7,8].

PMT is the major toxin of *Pasteurella multocida*, which colonizes the gastrointestinal tract and nasopharynx of animals like cats, dogs and pigs [9]. This toxin is the causative agent of progressive atrophic rhinitis in pigs, which is characterized by the loss of nasal turbinate bones [10,11]. After entering of target cells, the toxin deamidates an essential glutamine residue in the switch II region of Gα subunits of heterotrimeric G proteins resulting in glutamic acid [12,13]. This modification blocks the intrinsic GTPase activity of the G protein rendering the protein constitutively active. PMT is able to act on $G\alpha_{q/11}$, $G\alpha_{12/13}$, and $G\alpha_i$, whereas $G\alpha_s$ is not activated by the toxin [13,14]. The constitutive activation of heterotrimeric G proteins has profound consequences on bone metabolism. In previous studies, we showed that PMT inhibits the differentiation and/or function of osteoblasts by activating $G\alpha_{q/11}$ in pre-osteoblasts [15]. At the same time, PMT induces osteoclastogenesis by directly acting on osteoclast precursor cells as shown in bone marrow derived CD14+ monocytes and RAW246.7 cells [16]. These actions provide a rationale for the bone loss as observed in atrophic rhinitis in pigs.

Here, we studied the impact of heterotrimeric G protein signaling on osteoblastogenic markers in a cell culture model of FOP by using C2C12 myoblast cells, which were engineered to express Alk2(R206H). In this cell model, both BMP-4 and the patho-physiological agonist Activin A stimulated osteoblastogenesis-like differentiation, which we determined both by studying ALP activity as an early differentiation marker [17] and by measuring osteoblast-associated gene expression. We report that PMT strongly inhibited BMP-4- and Activin A-stimulated increase in ALP activity by activation of G_q proteins. Moreover, we show that activation of G_q signaling via adrenoceptors blocked ALP activity in these cells.

2. Results

2.1. C2C12 cells are efficiently intoxicated by PMT

One established cellular model of FOP is C2C12, a mouse myoblast cell line [18,19], which is able to differentiate to osteoblasts when incubated with osteogenic BMPs [20]. We intoxicated C2C12 cells overnight with PMT or the catalytically inactive mutant PMT^{C1165S}. Deamidation of heterotrimeric G proteins was determined in immunoblot studies using a monoclonal anti-GαQE antibody, which specifically detects deamidation of glutamine-209 in $G\alpha_q$ and glutamine-204/205 in $G\alpha_i$ [13,21,22]. PMT but not PMT^{C1165S} led to a distinct band at a molecular weight of ~40 kDa (Fig. 1A). This finding was confirmed in

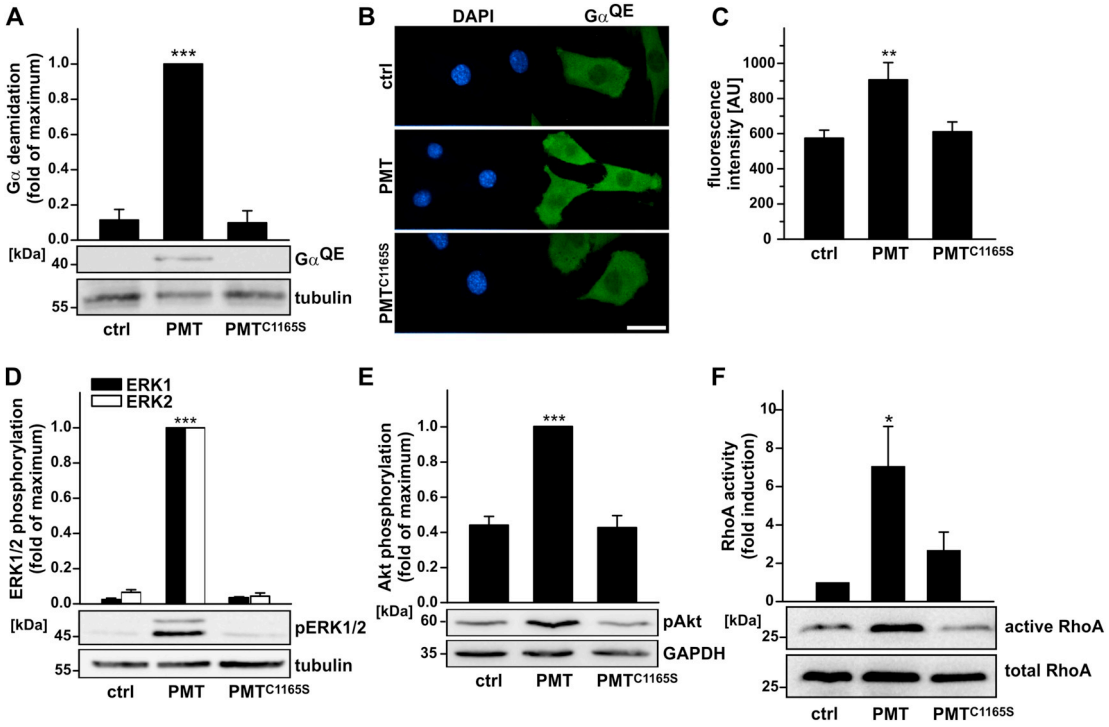

Fig. 1. Susceptibility of C2C12 cells to PMT. Gα-deamidation after incubating C2C12 cells with 1 nM PMT/PMT^{C1165S} for 16 h is shown in immunoblot (**A**) and immunofluorescence (**B/C**) experiments. **A** Deamidation of Gα was detected in cellular lysates in immunoblot analysis using a deamidation-specific anti-GαQE antibody. A representative immunoblot from 3 independent experiments is shown. Tubulin was used as loading control. The corresponding quantifications represent mean values and SEM relative to maximum values. **B** Immunofluorescence images from confocal microscopy show deamidated Gα (green) and nuclei of the cells (blue). Representable pictures from one of 3 independent experiment are shown (scale bar = 30 µm). **C** Quantification of immunofluorescence pictures. Means and SEM are shown of 3 independent experiments (15 fields of view for each condition). (AU: arbitrary units) **D/E** ERK1/2 and Akt phosphorylation after incubating C2C12 cells with 1 nM PMT/PMT^{C1165S} for 16 h and subsequently serum starving them for 1 h. Panels show representative immunoblots from at least 3 independent experiments with tubulin or GAPDH as loading controls. The corresponding quantifications represent mean values and SEM relative to maximum values. **F** RhoA activity after incubation of C2C12 cells with 1 nM PMT/PMT^{C1165S} for 4 h. The picture represents a representative blot from 4 independent effector-pulldown assays using total RhoA as a loading control. Means and SEM are shown. A larger fraction of blots displayed in Fig. 1 can be found in Fig. S1A-C. (For interpretation of the references to color in this figure legend, the reader is referred to the web version of this article.)

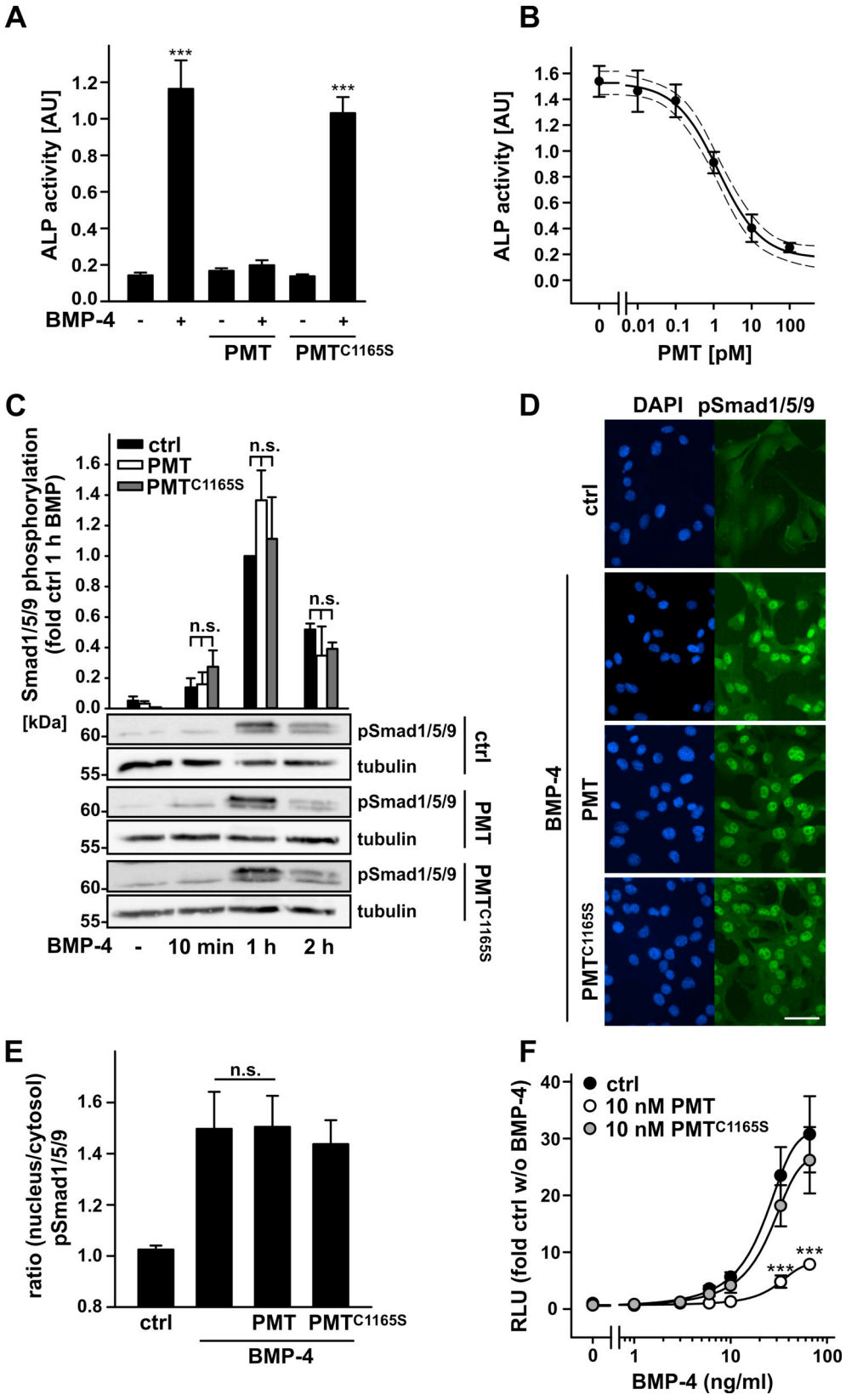

Fig. 2. Effects of PMT on ALP activity and Smad signaling. **A** Alkaline phosphatase (ALP) activity after incubating C2C12 cells for 5 d with 100 ng/ml BMP-4 with/without 100 pM PMT/PMT^{C1165S}. Means and SEM (n = 3) are shown. **B** PMT efficiency (ALP activity assay) after incubating C2C12 cells for 5 d with 100 ng/ml BMP-4 and indicated concentrations of PMT. Means and SEM (n = 3) are shown. The dotted line represents the 95% confidence interval of the non-linear regression. An EC_{50} (inhibition of ALP activity by PMT) of 1.2 pM was calculated from the regression. **C** Analysis of Smad1/5/9 phosphorylation by immunoblotting after intoxication of C2C12 cells with 1 nM PMT/PMT^{C1165S} for 16 h and further incubation with 100 ng/ml BMP-4 for indicated durations. Tubulin is used as a loading control. Means and SEM (n = 3) are depicted relative to control cells treated with BMP-4 for 1 h. The panels show representative immunoblots from 3 independent experiments. **D** Immunofluorescence images show phosphorylated Smad1/5/9 (green) and nuclei of the cells (blue). Cells were intoxicated with 1 nM PMT/PMT^{C1165S} for 16 h and then incubated with 100 ng/ml BMP-4 for 1 h. Representative images from one of 3 independent experiments are shown (scale bar = 20 μm). **E** Quantification of microscopic images. Nucleus/cytosol fluorescence intensity ratios are depicted as means and SEM (n = 3; at least 25 cells analyzed per experiment and condition). **F** The effects of PMT on BMP-dependent transcriptional activity was measured in a dual luciferase system. One day after transfection with luciferase constructs (see Materials and methods), C2C12 cells were incubated with 10 nM PMT/PMT^{C1165S} for 16 h and then stimulated with indicated concentrations of BMP-4 for 6 h. Means and SEM (n = 3) are depicted relative to untreated controls (***: statistical significance compared to BMP-4 concentration-matched controls, RLU: relative light units). A larger part of the blots shown in Fig. 2 can be found in Fig. S1D. (AU: arbitrary units (absorption at 405 nm normalized to cell numbers)). (For interpretation of the references to color in this figure legend, the reader is referred to the web version of this article.)

immunofluorescence studies with the anti-QE antibody, showing that treatment of C2C12 cells with PMT resulted in an increase in fluorescence intensity compared to untreated controls or cells treated with PMT^{C1165S} (Fig. 1B, C). In line with an activation of G proteins, PMT induced ERK1/2 (Fig. 1D) and Akt (Fig. 1E) phosphorylation and stimulated the activation of the small GTPase RhoA as measured by an effector (rhotekin) pull-down assay (Fig. 1F). Thus, as shown previously for osteoblasts [23], C2C12 cells are a cellular model, which is susceptible for PMT.

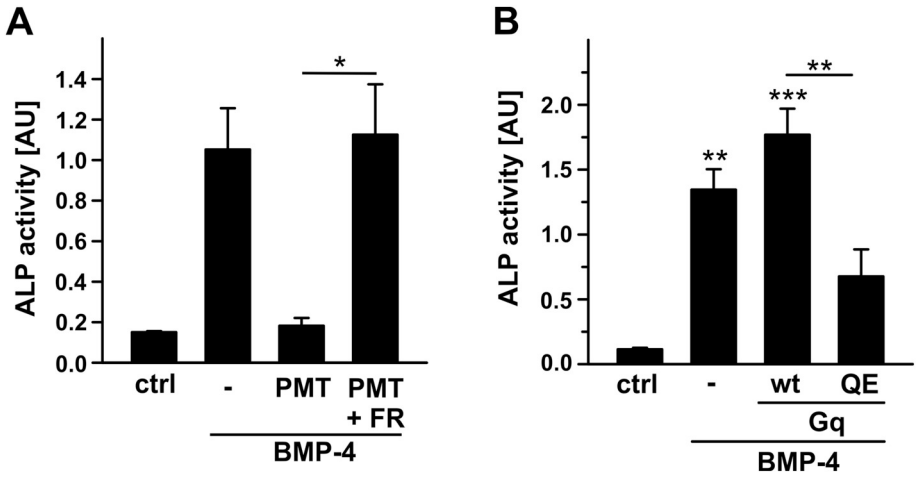

Fig. 3. Inhibition of ALP activity by activation of G_q signaling. **A** ALP activity after incubating C2C12 cells for 5 d with 100 ng/ml BMP-4 and 100 pM PMT with/without 100 nM FR900359. Means and SEM (n = 3) are depicted. **B** ALP activity after (over)expressing a wild type (wt) or a constitutively active (QE) version of $G\alpha_q$ in C2C12 cells and then stimulating the cells with 100 ng/ml BMP-4 for 5 d. Means and SEM (n = 3) are shown. (AU: arbitrary units (absorption at 405 nm normalized to cell numbers)).

2.2. PMT inhibits BMP-4-mediated increase in alkaline phosphatase (ALP) activity

Next, we studied osteoblast differentiation of C2C12 cells by measuring ALP activity, which is an early marker for osteoblastogenesis [17]. Treatment of cells with BMP-4 for 5 days caused 8fold increase in ALP activity suggesting differentiation of C2C12 cells to osteoblasts. This increase in ALP activity induced by BMP was completely inhibited by PMT but not by the inactive mutant PMT^{C1165S} (Fig. 2A). Notably, we determined an EC_{50} of 1.2 pM for inhibition of ALP activity by PMT, indicating the high potency of the toxin (Fig. 2B). Smad proteins (Smad1/5/9) are involved in the downstream signaling of Alk2, they are phosphorylated in their carboxy-terminal SSXS motive subsequently to BMP receptor activation and then translocate into the nucleus (reviewed in [24,25]). Therefore, we were prompted to study whether PMT has any effect on the phosphorylation of Smad1/5/9 proteins or on nuclear translocation. As shown in Fig. 2C–E, we did not observe a change of the phosphorylation of Smad1/5/9 by PMT. Furthermore, PMT had no effects on their nuclear localization. However, PMT decreased the expression of a BMP response element (BRE)-luciferase construct, which suggests that the toxin decreases BMP-dependent gene expression (Fig. 2F).

2.3. G_q signaling inhibits BMP-4-mediated increase in ALP activity

Previously, it has been shown that the effect of PMT on bone cell

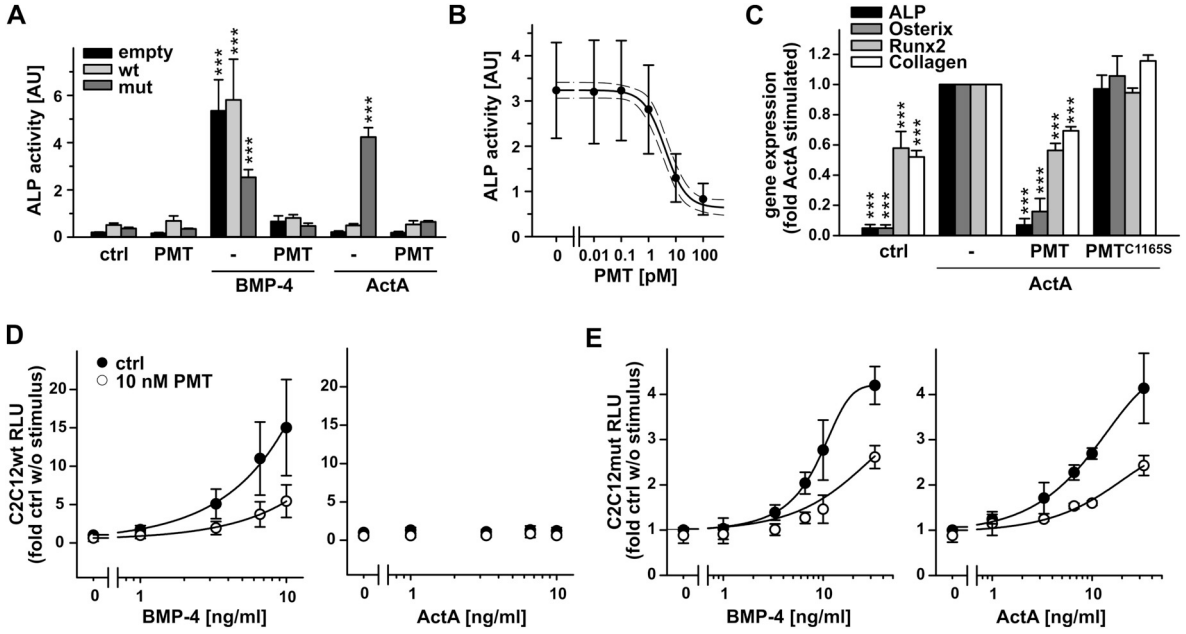

Fig. 4. Inhibition of osteoblastogenesis markers by PMT in C2C12-Alk2(R206H) cells. C2C12 cells were transduced with the FOP-variant of Alk2 bearing the R206H mutation. A stable cell line was generated as described in the Materials and methods section. **A** Alkaline phosphatase (ALP) activity after incubating C2C12wt and C2C12-Alk2(R206H) (mut) cells for 5 d with 100 ng/ml BMP-4 or Activin A with/without 100 pM PMT/PMT^{C1165S}. Means and SEM (n = 3) are shown. **B** PMT efficiency (ALP activity assay) after incubating C2C12mut cells for 5 d with 100 ng/ml Activin A and indicated concentrations of PMT. Means and SEM (n = 3) are depicted. The dotted line represents the 95% confidence interval of the non-linear regression. An EC_{50} (inhibition of ALP activity by PMT) of 4.1 pM was calculated from the regression. **C** The expression of osteogenic markers after incubating C2C12 Alk2-R206H cells for 5 d with 100 ng/ml Activin A with/without 100 pM PMT/PMT^{C1165S} was determined by RT-qPCR analysis. Means and SEM (n = 3) of expression levels of ALP, osterix, Runx2 and collagen1A2 are shown relative to Activin A-stimulated samples. **D/E** The effects of PMT on BMP- and Activin A-dependent transcriptional activity is measured using dualluciferase system in C2C12wt and C2C12mut cells. One day after transfection with luciferase constructs, cells were incubated with 10 nM PMT for 16 h and then stimulated with indicated concentrations of BMP-4 or Activin A for 6 h (described in detail in the Materials and methods section). Means and SEM (n = 3) are depicted relative to untreated controls (RLU: relative light units; AU: arbitrary units (absorption at 405 nm normalized to cell numbers)).

metabolism is mainly based on its action on $G\alpha_{q/11}$ signaling [15,16]. To elucidate whether $G\alpha_q$ is also a key player in PMT-induced inhibition of ALP activity in C2C12 cells, we employed the specific $G\alpha_q$ inhibitor FR900359. The addition of FR900359 completely inhibited the PMT effect and allowed an increase in ALP activity after stimulation by BMP-4 (Fig. 3A). Moreover, to mimic the effect of PMT, we expressed the constitutively active $G\alpha_q$ Q209E mutant in C2C12 cells. $G\alpha_q$ Q209E but not expression of wild type (wt) $G\alpha_q$ blocked an increase in ALP activity (Fig. 3B). These data suggest that activation of G_q signaling is sufficient to inhibit osteoblast-related differentiation, which was determined in our model system by measuring ALP activity.

2.4. PMT inhibits Activin A-mediated induction of osteoblast markers in FOP model cells

To test the capability of PMT to inhibit the induction of osteoblast markers in the context of a FOP cell model, we expressed Alk2wt (wt) and the FOP mutation Alk2(R206H) (mut) under the control of a doxycycline-responsive promoter in C2C12 cells. Doxycycline-induced expression of wild type or mutant Alk2 was monitored by RFP fluorescence (Fig. S2). In all following experiments, doxycycline was added to cell culture medium to induce expression of the indicated versions of Alk2 and at the same time RFP.

C2C12wt, C2C12mut, and C2C12empty (transduced with empty pFRIPZ) cells showed increased ALP activity in response to BMP-4 (Fig. 4A). The observed increase in ALP activity was strongly inhibited by PMT (Fig. 4A). Under normal conditions, the Alk2 antagonist Activin A dampened BMP-4-induced expression of the BRE-luciferase construct (Fig. S3) suggesting that Activin A normally counteracts BMP-4-induced osteoblast-related differentiation. However, Activin turns into an Alk2 agonist in the context of FOP and was therefore able to induce an increase in ALP activity in C2C12mut cells but not in C2C12wt and C2C12empty cells (Fig. 4A). Notably, PMT inhibited both Activin A- and BMP-4-induced ALP activity (Fig. 4A, B). The EC_{50} value (4.1 pM) of PMT-mediated inhibition of Activin A-induced ALP activity was in the same range as the inhibition for BMP-4-induced osteoblast

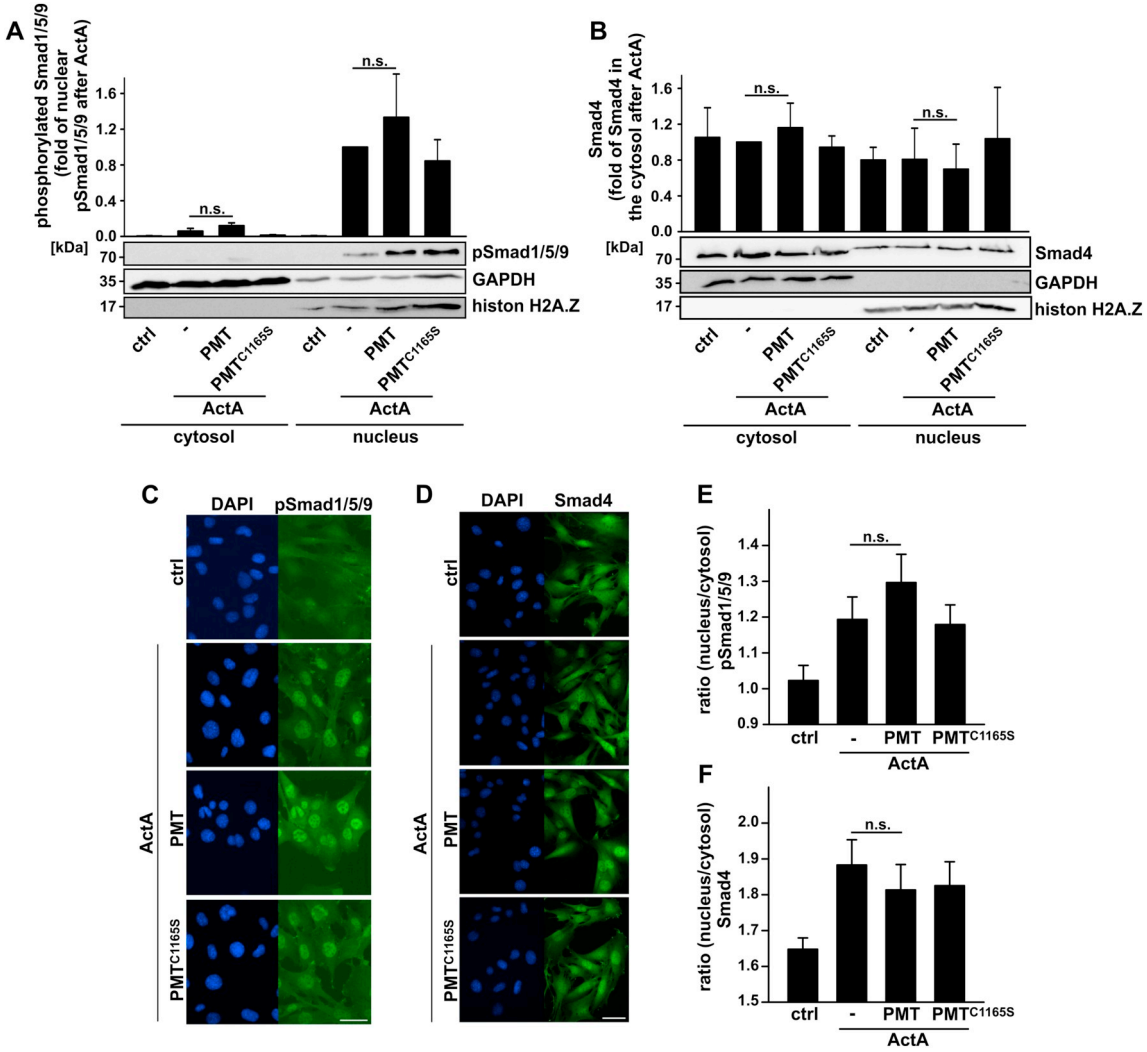

Fig. 5. Effects of PMT on nuclear translocation of the Smad complex. **A/B** Localization of phosphoSmad1/5/9 and Smad4 in nuclear and cytosolic fractions of the cell lysate. Analysis by immunoblotting after intoxication of C2C12mut cells with 1 nM PMT/PMT^{C1165S} for 16 h and further incubation with Activin A for 40 min. GAPDH and histonH2A.Z were used as a loading controls for the cytosolic and nuclear fractions, respectively. Panels show representative blots from at least 3 independent experiments. Means and SEM (n = 3) are depicted relative to nuclear (for phosphoSmad1/5/9) or cytosolic (for Smad4) fraction treated with Activin A only. **C/D** Immunofluorescence images show phosphoSmad1/5/9 and Smad4 in green and nuclei in blue. Cells were intoxicated with 1 nM PMT/PMT^{C1165S} for 16 h and then incubated with 100 ng/ml Activin A for 1 h. Representative images from one of 3 independent experiments are shown (scale bars = 20 µm). **E/F** Quantification of microscopic images. Nucleus/cytosol fluorescence intensity ratios are depicted as means and SEM (n = 3; at least 15 cells analyzed per experiment and condition). Larger parts of the blots shown in Fig. 5 can be found in Fig. S1E-F. (For interpretation of the references to color in this figure legend, the reader is referred to the web version of this article.)

differentiation in C2C12wt cells (Fig. 4B).

Furthermore, the influence of Activin A on the expression of a panel of osteogenic markers was determined 5 days after incubation of C2C12mut cells with Activin A. Activin A increased the expression of alkaline phosphatase (ALP), osterix, Runx2 and collagen1A2 as compared to undifferentiated control cells (Fig. 4C). PMT but not the inactive mutant PMT^{C1165S} attenuated the expression of osteoblast markers (Fig. 4C). In line with these findings, both BMP-4 and Activin A induced the expression of a BRE-luciferase construct in a concentration-dependent manner in C2C12mut cells but only BMP-4 and not Activin A was able to stimulate the expression of the reporter construct in C2C12wt cells (Fig. 4D, E). Notably, PMT diminished luciferase expression under all conditions (Fig. 4D, E).

To assure that the induction of the BRE-construct solely relies on binding of the Smad complex to its distinct response elements (AGAC), the respective sequences were mutated to ACTC (Fig. S4A). Using this mutant BRE-construct, stimulation of luciferase activity by Activin A was negligible (Fig. S4B). Thus, luciferase expression depended exclusively on R-Smad-signaling, which was modulated by PMT.

2.5. PMT does not alter cellular Smad localization in response to Activin A

Stimulation of C2C12mut cells with 100 ng/ml Activin A for 40 min caused nearly complete nuclear localization of phosphorylated Smad1/5/9 (Fig. 5A). However, PMT had no effect on the efficiency of nuclear accumulation of the Smad complex (Fig. 5A). In line with these results, confocal microscopy analysis of C2C12mut cells intoxicated with PMT for 16 h, followed by Activin A stimulation revealed a strong localization of phospho-Smad1/5/9 in the nucleus (Fig. 5C, E).

Finally, we also investigated nuclear localization of Smad4, which binds to R-Smads and enables them to alter gene expression [25]. We did no detect any change in Smad4 localization in response to Activin A or PMT in immunoblot studies (Fig. 5B). In contrast, immunofluorescence analysis revealed a slight increase in nuclear translocation of Smad4 after treatment of C2C12mut cells with Activin A for 1 h (Fig. 5D, F). PMT, however, did not change nuclear accumulation of Smad4 (Fig. 5D, F).

2.6. G_q-Calcium signaling inhibits Activin A-mediated induction of ALP activity

To verify the involvement of $G\alpha_q$-signaling in PMT-mediated inhibition of osteoblast marker activation, we transduced C2C12mut cells with constitutively active versions of different Gα-proteins (Fig. S5). In cells expressing permanently active $G\alpha_q$, but not constitutively active versions of the other family members ($G\alpha_i$, $G\alpha_s$ and $G\alpha_{12}$), Activin A-mediated induction of ALP was strongly diminished (Fig. 6A). This suggests that $G\alpha_q$ is able to negatively regulate the osteoblast-like differentiation. In contrast, active $G\alpha_s$ further stimulated ALP activity (Fig. 6A). Also in C2C12mut cells, pharmacological inhibition of $G\alpha_{q/11}$ (FR900359) reversed the PMT-mediated inhibition ALP activity (Fig. 6B), providing additional evidence for the importance of G_q in PMT-mediated inhibition of ALP activity.

Further downstream of the G_q signaling pathway, $G\alpha_q$ activates phospholipase C (PLC) which - via the cleavage of PIP_3 - leads to a calcium release from intracellular storage compartments as the ER.

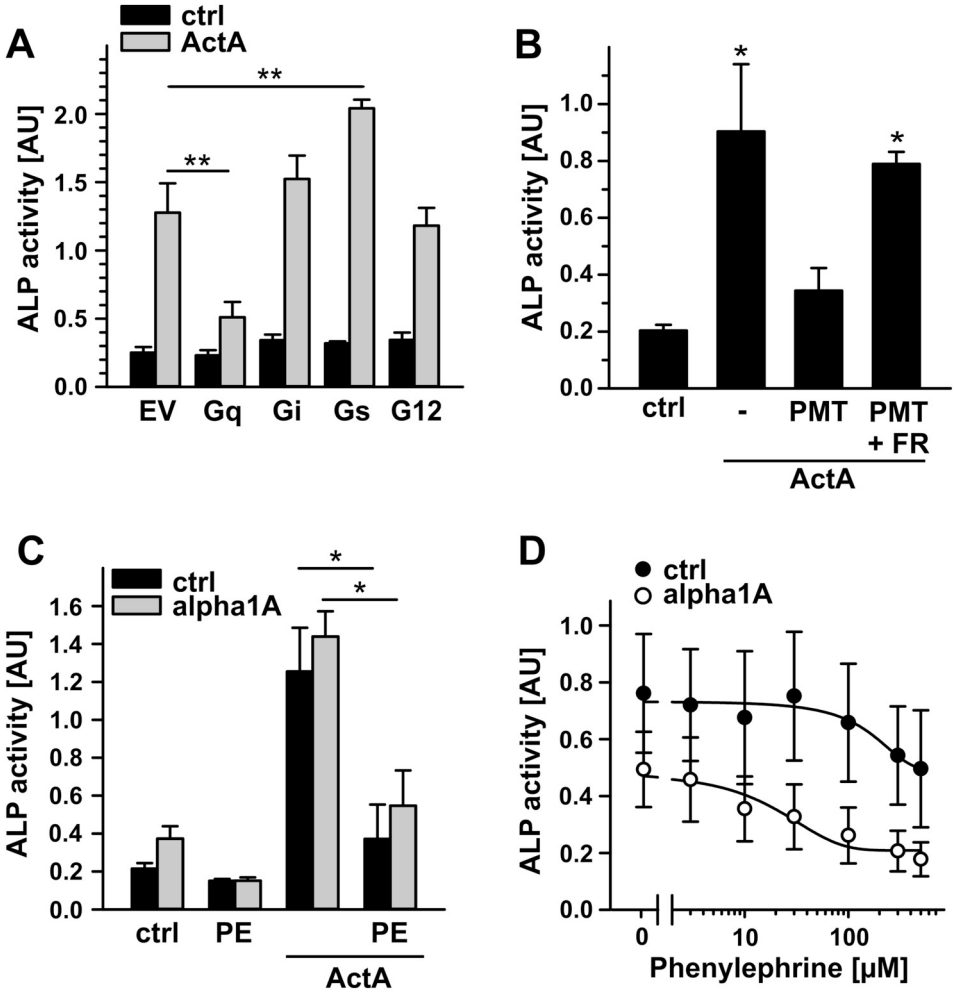

Fig. 6. Inhibition of ALP activity by activation of G_q signaling. **A** ALP activity after expressing constitutively active versions of Gα family members in C2C12mut cells and stimulating them with 100 ng/ml Activin A for 5 d. Means and SEM (n = 3) are shown. (EV: empty vector) **B** ALP activity after incubating C2C12mut cells for 5 d with 100 ng/ml Activin A and 100 pM PMT with/without 100 nM FR. Means and SEM (n = 3) are depicted. **C** ALP activity after incubating C2C12mut cells with 500 µM phenylephrine (PE) and stimulating the cells with 100 ng/ml Activin A for 5 d. Grey bars represent cells overexpressing α_1A-adrenergic receptor, black bars represent untransfected controls. Means and SEM (n = 3) are shown. **D** PE efficiency after incubating C2C12mut cells for 5 d with 100 ng/ml Activin A and indicated concentrations of PE. Open dots represent cells overexpressing α_1A-adrenergic receptor, black dots represent untransfected controls. Means and SEM (n = 3) are shown. (AU: arbitrary units (absorption at 405 nm normalized to cell numbers)).

Here, we demonstrate that the increase of cytoplasmic Ca^{2+} induced by the Calcium-ionophore A23187 both decreased ALP activity (Fig. S6B) and the expression of a BRE-luciferase-construct (Fig. S6A) when C2C12mut cells were additionally stimulated with Activin A. We show that activating PKC using PMA had the same effect in ALP activity and luciferase reporter assays as PMT or A23187 (Fig. S6C, D). Furthermore, we demonstrate that PMT activates PKC (Fig. S6E), which identifies this pathway as a potential mechanism of action of PMT-mediated inhibition of ALP activity in our C2C12 FOP model cell line.

Last, we asked whether G_q-activation via GPCRs might also affect ALP activity. To this end, we employed phenylephrine (PE), which is an α_{1A}-adrenoceptor agonist, to activate G_q. Also, PE inhibited Activin A-induced increase in ALP activity in C2C12mut cells as observed for PMT (Fig. 6C). ALP activity was concentration-dependently decreased by PE in cells overexpressing the α_{1A}-adrenergic receptor and in C2C12mut cells not overexpressing this receptor (Fig. 6D).

3. Discussion

FOP is a highly disabling human disease with poor prognosis and limited therapeutic options [4]. Currently, no effective medical therapy is known. Prevention of injury and soft tissue trauma, and administration of bisphosphonates and corticosteroids during flare-ups to control inflammatory reactions are strategies to slow down disease progression [26]. A few years ago, it has been found that the classical Alk2 mutation in FOP (R206H) leads to an over-activation of the receptor by rendering it responsive to the normally inhibitory ligand Activin A [5,6].

Here, we show that C2C12 cells, which are frequently used as a FOP model cell line, are susceptible for the activity of PMT. Previously, the toxin had been shown to inhibit differentiation and activity of osteoblasts and increased activity and differentiation of osteoclasts [16,23]. In C2C12 cells, PMT potently and efficiently inhibited the BMP-4-induced increase in ALP activity, which we measured as a surrogate for osteoblastogenesis. PMT is known to activate G-proteins by deamidation [12,13]. We confirmed this specific deamidation of G proteins by PMT also in C2C12 cells. Our studies with a specific antibody that identifies the deamidation of a glutamine residue in the α-subunit of $G_{q/11}$, $G_{i/o}$ and $G_{12/13}$, demonstrate that G proteins are deamidated by PMT in C2C12 cells. However, in line with previous reports on the toxin's effects on differentiation of osteoblasts and osteoclasts, several data indicate that the activation of the $G_{q/11}$ protein appears to be predominant for inhibition ALP activity in C2C12 cells following activation by BMP-4. First, a specific inhibitor of $G_{q/11}$ blocked the effect of PMT. Moreover, expression of the persistently active $G\alpha_q$ mutant exhibited the same inhibitory effects in an ALP activity assay as PMT. However, the functional connection between BMP-receptor signaling and activation of G_q remains elusive. PMT did not affect phosphorylation of the SSXS motif in Smad1/5/9. Also, the translocation of Smads into the nucleus was not affected by PMT. Interestingly, the toxin significantly reduced the transcription activity of the BMP responsive element determined with a selective reporter construct which might suggest a decreased efficiency in binding of the Smad complex to its target DNA sequence.

To improve the C2C12 cell culture-FOP model, we expressed Alk2, containing the classical FOP mutation (R206H), in these cells under the control of a doxycycline-dependent promoter. Results obtained with C2C12 cells expressing Alk2(R206H) are fully in line with the hypothesis that both BMP-4 and the patho-physiological ligand Activin A induced the differentiation to osteoblasts, which was determined both by ALP activity measurements and the induction of Smad1/5/9-signaling. Notably, Activin A caused an increase in ALP activity and expression of a BRE-luciferase construct only in cells with the Alk2(R206H) mutant but not in wildtype cells. PMT did not only inhibit BMP-4-induced osteoblastogenesis-related differentiation but also counteracted Activin A-mediated activation of osteoblast markers. This was demonstrated both by a decreased alkaline phosphatase activity as well as decreased expression of the osteogenic markers collagen1A2, Runx2 and osterix in response to the toxin. Consequently, PMT is able to block osteoblast-like differentiation induced by Activin A in a FOP-relevant cellular model.

We further found that the overexpression of active $G\alpha_q$, an increase in intracellular Ca^{2+} by the ionophore A23187 and an activation of PKC by PMA had the same effect on ALP activity and Smad1/5/9-dependent gene expression as PMT, suggesting that G_q-dependent signaling cascades may be responsible for PMT-mediated inhibition of osteoblast-like differentiation. Most importantly, also the activation of a G_q-coupled GPCR, α_{1A}-adrenoceptor, was sufficient to inhibit ALP activity in our FOP cell model. In line with these findings, previous works have shown impaired osteoblast differentiation and severe osteopenia in mice expressing a constitutively active version of $G\alpha_q$ (Q209L) in the osteoblast lineage [27]. PKC has been proposed as important player in inhibition of osteoblast differentiation [27–29]. Thereby, PKC stabilizes Msx2 protein, which in turn negatively regulates osteoblast differentiation by suppressing transcriptional activity of Dlx5, a key transcription factor in osteoblastogenesis [28,30].

In our study, however, the crosstalk between BMP-Smad signaling and GPCR-G_q-calcium signaling remains elusive. We show that PMT did not alter receptor Smad1/5/9 phosphorylation or translocation of the activated Smad complex into the nucleus but decreased the BMP/Activin A-dependent expression of a BRE-luciferase reporter construct. Moreover, PMT inhibited Activin A-induced expression of a panel of osteoblast markers. The osteogenic transcription factor Dlx5 has been reported to be directly regulated by the BMP-Smad-cascade; Dlx5 mRNA increases after BMP treatment of cells without the need of further protein synthesis [28]. In a subsequent study it would be worth testing the impact of PMT on Dlx5 synthesis and Msx2. It would be interesting to challenge the hypothesis that PMT suppresses Dlx5 synthesis by decreasing the efficiency of BMP-Smad-dependent gene expression. Additionally, PMT might stabilize Msx2 via the activation of PKC leading to an even stronger suppression of osteoblast marker gene expression.

Although the molecular mechanism is not fully understood yet, our study provides plenty of evidence that the activation heterotrimeric G proteins and especially of G_q-signaling might be a novel therapeutic approach in the treatment of FOP. This is of great relevance because GPCRs are highly druggable which is mirrored by the fact that ca. 35% (475 compounds) of all drugs approved by the US Food and Drug Administration (FDA) act on 108 different GPCRs [31]. Therefore, screening of already clinically approved GPCR agonists might be considered as method to find novel therapeutic concepts for FOP. The introduction of an effective drug to treat this severe condition is urgently needed and the possibility of drug repositioning would critically shorten the approval procedure compared to a completely new compound.

4. Materials and methods

4.1. Materials

C2C12 cells were obtained from Bioss (Centre for Biological Signaling Studies, Freiburg, Germany) Toolbox. Dulbecco's modified Eagle medium (DMEM) and fetal bovine serum (FBS) were obtained from Biochrom (Berlin, Germany). Recombinant BMP-4 and Activin A were purchased from Pepro-Tech (Hamburg, Germany). Oligonucleotides were obtained from Apara (Denzlingen, Germany) or biomers.net GmbH (Ulm, Germany). The $G\alpha_{q/11}$ inhibitor FR900359 was a gift from Prof. G. M. König and Prof. E. Kostenis. The calcium ionophore A23187 was purchased from Sigma-Aldrich (St. Louis, USA). PMA was obtained from Biomol (Hamburg, Germany). All other reagents were of analytical grade and purchased from commercial sources.

4.2. Cell culture and osteoblast differentiation

C2C12 cells were cultured in DMEM supplemented with 10% FCS, 100 units/ml penicillin, 100 µg/ml streptomycin, 1× non-essential amino acids and 1 mM sodium-pyruvate and kept at 37 °C, 5% CO_2 during all experiments. For osteoblast differentiation, cells were cultured in low-proliferation medium (DMEM with 5% FCS, 100 units/ml penicillin, 100 µg/ml streptomycin, 0.5× non-essential amino acids and 0.5 mM sodium-pyruvate) supplemented with 100 ng/ml BMP-4 or Activin A for 5 d.

4.3. Alkaline phosphatase activity

After 3 or 5 d of osteoblast differentiation, the early osteogenic marker alkaline phosphatase was detected. Cells were washed with PBS and incubated with 100 µl of assay solution (12 mM $MgCl_2$, 100 µM $ZnCl_2$, 100 mM Glycin-NaOH (pH 10.5), 8 mM *p*-Nitrophenylphosphate (added freshly prior to assay)) per 24 well for 10 min at 37 °C. The reaction was stopped by adding 100 µl 0.2 M NaOH to each well. Absorption was measured at 405 nm. For normalization to the number of viable cells in our samples, a CellTiter Blue assay (Promega; Mannheim, Germany) was performed according to manufacturer's instructions prior to alkaline phosphatase activity measurements.

4.4. Generation of C2C12-Alk2(R206H) cells

The classical FOP mutation 617G > A was introduced into the Acvr1 gene by site-directed mutagenesis. Wild type (wt) and 617G > A Acvr1 were cloned into the lentiviral and tetracycline-inducible vector pFRIPZ (a kind gift from Prof. Brummer, Freiburg). To control for expression of the target genes, RFP is expressed simultaneously via an IRES site. Lentiviruses were generated by transfecting HEK293T cells with a set of lentiviral packaging plasmids (pTLA1-Pak, pTLA1-Enz, pTLA-Env, pTLA-Tat/Rev, pTLA1-TOFF, all ThermoFisher; Waltham, USA) in addition to the pFRIPZ vector. C2C12 cells were transduced and selected using the puromycin-resistance gene encoded on the pFRIPZ vector for 4 weeks. In all experiments using C2C12-Alk2(R206H) cells (C2C12mut), doxycycline was added to induce the expression of Alk2(R206H).

4.5. Rhotekin pulldown assay

The detection of RhoA activation by Rhotekin pulldown assay was performed as described previously [32]. C2C12 cells were intoxicated for 4 h, washed 2 times with PBS and lysed with GST-fishbuffer. Then the lysates were incubated with Rhotekin beads on a rotating shaker for 1 h at 4 °C and the amount of bound active RhoA was determined by immunoblot analysis.

4.6. Immunoblot detection

For detection of G protein deamidation and effects of PMT on the phosphorylation status of ERK1/2, Akt and Smad1/5/9 in cell lysates, C2C12 cells were treated for 17 h with PMT or PMT^{C1165S} (1 nM). To assess the phosphorylation levels of ERK1/2 and Akt, cells were starved (culture medium with 1% FCS) for one hour prior to immunoblotting. To assess phosphorylation of PKC substrate, C2C12mut cells were intoxicated for 2, 4 or 6 h with PMT or PMT^{C1165S} (1 nM) or stimulated with PMA (200 nM) as positive control for 30 min. Additionally, cells were starved for 1 h prior to lysis. To verify the (over-) expression of different (constitutively active) G proteins, cells were lysed one week after transduction with the respective constructs.

For lysis, RIPA buffer (50 mM Tris-HCl pH 7.4, 1% Triton-X 100, 137.5 mM NaCl, % glycerol, 1 mM sodium orthovanadate, 0.5 mM EDTA pH 8, 0.5% sodium deoxycholate, 0.1% SDS) containing complete protease inhibitor and phosphatase inhibitor cocktails II and III (Sigma Aldrich; Taufkirchen, Germany) was used. Protein concentrations in the lysates were determined by the Bradford method. 50 to 70 µg of total protein were loaded per lane of the SDS-polyacrylamide gel, whereby the same protein amounts were loaded to each lane within each experiment. Lysates were separated using SDS-PAGE and the proteins were transferred onto polyvinylidene (PVDF)-membranes. The monoclonal rat anti-$G\alpha_q$ Q209E (3G3) was a kind gift of Dr. Y. Horiguchi. The antibody against phospho-p44/42 MAPK (Erk1/2) (Thr202/Tyr204) (#4370 (D13.14.4E)), phospho-Akt (Ser473) (#4060), the phosphospecific Smad1/5/9 (#9511) antibody and the antibody against phosphorylated PKC substrate (#2261) were purchased from Cell Signaling (Frankfurt, Germany). Antibodies against Galpha i-2 (sc7276), Galpha q/11 (sc392), Galpha s/olf (sc383) and Galpha 12 (sc409) were purchased from Santa Cruz (Heidelberg, Germany). Anti-tubulin- (T9026; Sigma Aldrich; Taufkirchen, Germany) or anti-GAPDH- (MAB374 (6C5); ThermoFisher; Waltham, USA) antibodies were used as loading controls. For visualization, the binding of the second horseradish peroxidase-coupled antibody was detected with an enhanced chemiluminescent detection reagent (SignalFire ECL Reagent; NEB, Frankfurt am Main, Germany). The imaging system LAS-3000 (Fujifilm; Düsseldorf, Germany) was used and the quantifications were done using MultiGauge software.

4.7. Cell fractionation

For each examined condition, cells from 2 10 cm-plates (confluency ca. 80%) were lysed on ice using 250 µl of fractionation buffer (250 mM sucrose, 20 mM HEPES, 10 mM KCl, 1.5 mM $MgCl_2$, 1 mM EDTA, 1 mM EGTA, 1 mM DTT, 1× complete protease inhibitor, phosphatase inhibitor cocktail II and III (Sigma Aldrich; Taufkirchen, Germany)) per plate. Cells were collected, passed through a 25 G needle 10 times, and left on ice for 20 min. The nuclear pellet was centrifuged out (750*g*, 5 min, 4 °C; supernatant was collected and represents the cytosolic fraction) and taken up in 500 µl fractionation buffer again, passed through a needle again 10 times and centrifuged as described above for 10 min. The nuclear pellet was resuspended in nuclear buffer (50 mM Tris-HCl pH 7.4, 1% Triton-X 100, 137.5 mM NaCl, 10% glycerol, 1 mM sodium orthovanadate, 0.5 mM EDTA pH 8, 0.5% sodium deoxycholate, 0.1% SDS, 1× complete protease inhibitor, phosphatase inhibitor cocktail II and III (Sigma Aldrich; Taufkirchen, Germany)), and sonicated briefly. The cytosolic fraction was centrifuged (10,000*g*, 5 min, 4 °C). The supernatant was concentrated by centrifuging through a filter unit with 10 kDa cutoff (Millipore; Darmstadt, Germany). Protein concentrations in both the cytosolic and nuclear fractions were determined by the Bradford method to ensure loading of each lane in the gel with equal protein amounts. Lysates were separated using SDS-PAGE (50 to 70 µg of total protein per lane) and the proteins were transferred onto polyvinylidene (PVDF)-membranes. The localization of Smads was detected using the anti-Smad4 antibody (#46535 (D3R4N)) and the phosphospecific Smad1/5/9 (#9511) antibody from Cell Signaling (Frankfurt, Germany). The mouse anti-GAPDH antibody, (MAB374 (6C5); ThermoFisher; Waltham, USA) and the rabbit anti-Histone H2A.Z antibody (#2718S; Cell Signaling; Frankfurt, Germany) were used as loading controls for the cytosolic and nuclear fractions, respectively. Visualization was done as described above.

4.8. Retroviral transduction of C2C12 cells

pcDNA plasmids encoding $G\alpha_q$, $G\alpha_s$ (short version), $G\alpha_{i2}$, and $G\alpha_{12}$ (all with internal EE-tag) and α_1A-adrenergic receptor were obtained from the “cDNA Resource Center” (www.cdna.org). The DNA were inserted into pMIG vector via TOPO cloning (ThermoFisher; Waltham, USA). To generate active versions of the G proteins, point mutations were introduced via quickchange PCR resulting in an exchange of glutamine to glutamate as induced by PMT via deamidation (G_qEE C625G, G_{i2}EE C613G, G_sEE C637G, G_{12}EE C691G). 1.8×10^6 φNXeco

cells were seeded per 10 cm dish and grown for 24 h. Then they were transfected with 3 μg of pMIG vectors in 500 μl of plain DMEM containing 24 μg PEI (polyethylenimine) per 10 cm dish. 24 h after transfection, medium was replaced by 5 ml fresh culture medium. Cells were incubated for additional 48 h to allow production of viral particles. Viral particles-containing medium was filtered through a 0.45 μm pore size filter and was used immediately for infection of C2C12 cells or was stored at 4 °C for up to one week. For transduction of C2C12 or C2C12mut cells, medium was replaced by a mixture of two parts C2C12 medium and one part virus-containing filtered medium containing 8 μg/ml polybrene. The procedure was repeated 24 h after the first transduction to increase infection rates. 24 h after the second infection, cells were seeded for respective experiments.

4.9. Gene reporter assay

Activity of BMP-dependent protein expression was measured by the use of a dualluciferase reporter assay system (Promega; Mannheim, Germany). C2C12 cells were seeded in a 48-well plate and allowed to adhere overnight. Cells were then incubated for 24 h with a mixture of 0.125 μg of *Renilla* luciferase plasmid (pRL-TK; Promega; Mannheim, Germany) and 0.125 μg pGL3 firefly luciferase reporter plasmid, 0.5 μl Lipofectamine 2000 (ThermoFisher, Waltham, USA) and 25 μl Opti-MEM per well. Medium was changed to culture medium with reduced FCS (2.5%), 10 nM PMT was added and incubated for another 16 h. Afterwards, cells were incubated with BMP-4 or Activin A for 6 h before lysis and luciferase activity detection.

pGL3-BRE was obtained from Addgene (plasmid 45126; deposited by Martine Roussel, Peter ten Dijke). The pGL3-BREmut plasmid as well as the empty pGL3 vector was a kind gift from Prof. A. Hecht and Patrick Frey (University of Freiburg, Germany).

To engineer the pGL3-BREmut plasmid, a single-stranded, palindromic BRE-SBEmut oligonucleotide (ctagcTCACTCCGTTACTCGCCAG GACGGGCTGTCAGGCTGGCGCCGCGGCGCCAGCCTGACAGCCCGTCCT GGCGAGTAACGGAGTGAg, lowercase letter represent NheI restriction site overhangs) was heated to 99 °C for 10 min with a mixture of 200 pmol oligonucleotides, 10 μl of restriction enzyme buffer NEB-2 (NEB; Ipswich, USA) and 88 μl of water. Then, the mixture was gradually cooled down to room temperature. The resulting double-stranded DNA fragment was phosphorylated using T4 polynucleotide kinase (NEB; Ipswich, USA) according to the manufacturer's recommendations. Subsequently, the fragment was cloned into the pGL3-Luc backbone via the NheI restriction site.

4.10. Quantification of mRNA levels

To detect expression levels of osteogenic marker genes, total RNA was purified from C2C12mut cells using the RNeasy Mini Kit (Qiagen; Hilden, Germany) and transcribed in cDNA using QuantiTect Reverse Transcription Kit (Qiagen; Hilden, Germany) according to manufacturer's instructions. GoTaq qPCR Master Mix (Promega; Mannheim, Germany) was used for quantitative PCR. As an internal control expression levels of mouse ribosomal Protein S29 were measured. Fold changes were calculated using the LinRegPCR method [33,34]. For analysis following primer pairs were used: mS29 (forward-ATGGGTC ACCAGCAGCTCTA, reverse-AGCCTATGTCCTTCGCGTACT), mALP (forward-CACCCGAGTGGTAGTCACAA, reverse-AATGAGGTCACATCC ATCCTG), mSP7 (Osterix) (forward-CTCCTGCAGGCAGTCCTC, reverse-GGGAAGGGTGGGTAGTCATT), mRunx2 (forward-TGCCCAGGCGTAT TTCAG, reverse-TGCCTGGCTCTTCTTACTGAG), mCollagen1A2 (forward-GCAGGTTCACCTACTCTGTCCT, reverse-CTTGCCCCATTCATTTG TCT).

4.11. Confocal microscopy

Cells grown on coverslips were intoxicated with PMT or PMT^{C1165S} (1 nM) for 17 h and were then incubated with BMP-4 or Activin A for 1 h. Cells were fixed using 4% paraformaldehyde in PBS for 15 min at room temperature, washed three times with PBS and were then incubated with 100% Methanol at −20 °C for 10 min. Cells were washed once with PBS and then incubated overnight in a light-tight box at 4 °C with primary antibody (Smad4 or phosphospecific Smad1/5/9 antibody (as described above)), diluted in antibody solution (PBS, 1% BSA, 0.3% Triton-X-100). Then, cells were rinsed again tree times with PBS before they were incubated with fluorochrome-conjugated secondary antibody (AlexaFluor 488 chicken anti-rabbit; A21441, Invitrogen; Darmstadt, Germany) diluted in antibody solution for 1–2 h at room temperature in the dark. Cells were again washed three times with PBS. Then, the coverslips were mounted onto microscope slides using a mounting solution containing Mowiol and DAPI (prewarmed to 55 °C). The slides were left to dry overnight at 4 °C. Pictures were taken using confocal microscopy (microscope: Observer Z1, Zeiss; Oberkochen, Germany, equipped with confocal scanner unit CSU-X1, Yokogawa; Musashino, Japan; objective: EC Plan-Neofluar 40×/1.3 Oil, Zeiss; Oberkochen, Germany) with 40× magnification. Per condition, at least 5 pictures were taken. Nucleus/cytosol-intensity ratios were calculated using the MetaMorph Microscopy Automation and Image Analysis Software.

For visualizing deamidated Gα using the monoclonal rat anti-Gα_q Q209E (3G3)-antibody, C2C12 cells grown on coverslips were intoxicated with PMT or PMT^{C1165S} (1 nM) for 17 h before there were washed once and then fixed with 4% PFA in PBS for 12 min at room temperature. After three washes with PBS, cells were permeabilized using 0.15% Triton-X-100 in PBS for 10 min at room temperature. After three more washes, cells were blocked with 1% BSA in PBS-T (PBS, 0.05% Tween 20) for 30 min at room temperature. Then, cells were incubated for 3 h with primary antibody (anti-Gα_q Q209E (3G3)) diluted in PBS-T, 1% BSA and then washed again three times. Cells were then incubated with fluorochrome-coupled secondary antibody (AlexaFlour 488 goat anti-rat; A11006, Invitrogen; Mannheim, Germany) diluted in PBS-T for 1 h at room temperature. Finally, cells were washed three times with PBS and once with water before they were mounted as described above. Pictures were taken as described above using 100× magnification (objective: Plan-Apochromat 100×/1.4 Oil, Zeiss; Oberkochen, Germany). For quantification of fluorescence intensities, the area of the nuclei was excluded and intensities of the cytosolic part of cells were determined using the MetaMorph Microscopy Automation and Image Analysis Software.

4.12. PMT expression

Wild-type PMT (PMT) and the catalytically inactive mutant PMT^{C1165S} were expressed and purified as previously described [35].

4.13. Statistics

Results are presented as means ± SEM. Significance was assessed by ANOVA followed by Tukey's (Figs. 2C/E, 3A/B, 5A/B/E/F, 6A/C) or Dunnett's (Figs. 1A/D/E/F, 2A/F (F: respective concentration-matched controls), 4A/B (B: respective cells treated with Activin A only), 6B) post test. p values < 0.05 were considered statistically significant ($* = p < 0.05$, $** = p < 0.01$, $*** = p < 0.001$; n.s., not significant). Non-linear regressions were calculated in SigmaPlot using the 4 parameter logistic or sigmoid curve fit.

Declaration of Competing Interest

None.

Acknowledgement

We thank Dr. Y. Horiguchi (Osaka University, Japan) for deamidation specific antibody, Prof. T. Brummer (University of Freiburg,

Germany) for pFRIPZ vector and Prof. A. Hecht and Patrick Frey (University of Freiburg, Germany) for pGL3-BREmut and empty pGL3 vectors. Further, we thank Petra Bartholomé and Silke Fieber for excellent technical assistance. The study was financially supported by the Deutsche Forschungsgemeinschaft (DFG, OR218). E.K. and G.M.K. were supported by the Deutsche Forschungsgemeinschaft (DFG, FOR2372/1 and FOR2372/6).

Appendix A. Supplementary data

Supplementary data to this article can be found online at https://doi.org/10.1016/j.bone.2019.07.031.

References

[1] E.M. Shore, M. Xu, G.J. Feldman, D.A. Fenstermacher, T.J. Cho, I.H. Choi, J.M. Connor, P. Delai, D.L. Glaser, M. LeMerrer, R. Morhart, J.G. Rogers, R. Smith, J.T. Triffitt, J.A. Urtizberea, M. Zasloff, M.A. Brown, F.S. Kaplan, A recurrent mutation in the BMP type I receptor ACVR1 causes inherited and sporadic fibrodysplasia ossificans progressiva, Nat. Genet. 38 (5) (2006) 525–527.

[2] F.S. Kaplan, M. Le Merrer, D.L. Glaser, R.J. Pignolo, R.E. Goldsby, J.A. Kitterman, J. Groppe, E.M. Shore, Fibrodysplasia ossificans progressiva, Best Pract. Res. Clin. Rheumatol. 22 (1) (2008) 191–205.

[3] F.S. Kaplan, S.A. Chakkalakal, E.M. Shore, Fibrodysplasia ossificans progressiva: mechanisms and models of skeletal metamorphosis, Dis. Model. Mech. 5 (6) (2012) 756–762.

[4] F.S. Kaplan, D.L. Glaser, Thoracic insufficiency syndrome in patients with fibrodysplasia ossificans progressiva, Clinical Reviews in Bone and Mineral Metabolism 3 (2005) 213–216.

[5] S.J. Hatsell, V. Idone, D.M. Wolken, L. Huang, H.J. Kim, L. Wang, X. Wen, K.C. Nannuru, J. Jimenez, L. Xie, N. Das, G. Makhoul, R. Chernomorsky, D. D'Ambrosio, R.A. Corpina, C.J. Schoenherr, K. Feeley, P.B. Yu, G.D. Yancopoulos, A.J. Murphy, A.N. Economides, ACVR1R206H receptor mutation causes fibrodysplasia ossificans progressiva by imparting responsiveness to activin A, Sci. Transl. Med. 7 (303) (2015) 303ra137.

[6] K. Hino, M. Ikeya, K. Horigome, Y. Matsumoto, H. Ebise, M. Nishio, K. Sekiguchi, M. Shibata, S. Nagata, S. Matsuda, J. Toguchida, Neofunction of ACVR1 in fibrodysplasia ossificans progressiva, Proc. Natl. Acad. Sci. U. S. A. 112 (50) (2015) 15438–15443.

[7] C.L. Gregson, P. Hollingworth, M. Williams, K.A. Petrie, A.N. Bullock, M.A. Brown, J.H. Tobias, J.T. Triffitt, A novel ACVR1 mutation in the glycine/serine-rich domain found in the most benign case of a fibrodysplasia ossificans progressiva variant reported to date, Bone 48 (3) (2011) 654–658.

[8] F.S. Kaplan, M. Xu, P. Seemann, J.M. Connor, D.L. Glaser, L. Carroll, P. Delai, E. Fastnacht-Urban, S.J. Forman, G. Gillessen-Kaesbach, J. Hoover-Fong, B. Koster, R.M. Pauli, W. Reardon, S.A. Zaidi, M. Zasloff, R. Morhart, S. Mundlos, J. Groppe, E.M. Shore, Classic and atypical fibrodysplasia ossificans progressiva (FOP) phenotypes are caused by mutations in the bone morphogenetic protein (BMP) type I receptor ACVR1, Hum. Mutat. 30 (3) (2009) 379–390.

[9] I.W. Wilkie, M. Harper, J.D. Boyce, B. Adler, *Pasteurella multocida*: diseases and pathogenesis, Curr. Top. Microbiol. Immunol. 361 (2012) 1–22.

[10] E.M. Kamp, T.G. Kimman, Induction of nasal turbinate atrophy in germ-free pigs, using *Pasteurella multocida* as well as bacterium-free crude and purified dermonecrotic toxin of P multocida, Am. J. Vet. Res. 49 (11) (1988) 1844–1849.

[11] A.J. Lax, N. Chanter, Cloning of the toxin gene from *Pasteurella multocida* and its role in atrophic rhinitis, J. Gen. Microbiol. 136 (1) (1990) 81–87.

[12] J.H. Orth, I. Preuss, I. Fester, A. Schlosser, B.A. Wilson, K. Aktories, *Pasteurella multocida* toxin activation of heterotrimeric G proteins by deamidation, Proc. Natl. Acad. Sci. U. S. A. 106 (17) (2009) 7179–7184.

[13] J.H. Orth, K. Aktories, *Pasteurella multocida* toxin activates various heterotrimeric G proteins by deamidation, Toxins (Basel) 2 (2) (2010) 205–214.

[14] J.H. Orth, I. Fester, P. Siegert, M. Weise, U. Lanner, S. Kamitani, T. Tachibana, B.A. Wilson, A. Schlosser, Y. Horiguchi, K. Aktories, Substrate specificity of *Pasteurella multocida* toxin for α subunits of heterotrimeric G proteins, FASEB J. 27 (2) (2013) 832–842.

[15] P. Siegert, G. Schmidt, P. Papatheodorou, T. Wieland, K. Aktories, J.H. Orth, Pasteurella multocida toxin prevents osteoblast differentiation by transactivation of the MAP-kinase cascade via the Gα(q/11)–p63RhoGEF–RhoA axis, PLoS Pathog. 9 (5) (2013) e1003385.

[16] J. Strack, H. Heni, R. Gilsbach, L. Hein, K. Aktories, J.H. Orth, Noncanonical G-protein-dependent modulation of osteoclast differentiation and bone resorption mediated by *Pasteurella multocida* toxin, MBio 5 (6) (2014) e02190.

[17] R. Robison, The possible significance of hexosephosphoric esters in ossification (reprinted from Biochem J, Vol 17, Pg 286, 1923), Clin. Orthop. Relat. Res. (267) (1991) 2–7.

[18] D. Yaffe, O. Saxel, Serial passaging and differentiation of myogenic cells isolated from dystrophic mouse muscle, Nature 270 (5639) (1977) 725–727.

[19] H.M. Blau, G.K. Pavlath, E.C. Hardeman, C.P. Chiu, L. Silberstein, S.G. Webster, S.C. Miller, C. Webster, Plasticity of the differentiated state, Science 230 (4727) (1985) 758–766.

[20] T. Katagiri, A. Yamaguchi, M. Komaki, E. Abe, N. Takahashi, T. Ikeda, V. Rosen, J.M. Wozney, A. Fujisawa-Sehara, T. Suda, Bone morphogenetic protein-2 converts the differentiation pathway of C2C12 myoblasts into the osteoblast lineage, J. Cell Biol. 127 (6 Pt 1) (1994) 1755–1766.

[21] S. Kamitani, S. Ao, H. Toshima, T. Tachibana, M. Hashimoto, K. Kitadokoro, A. Fukui-Miyazaki, H. Abe, Y. Horiguchi, Enzymatic actions of *Pasteurella multocida* toxin detected by monoclonal antibodies recognizing the deamidated α subunit of the heterotrimeric GTPase Gq, FEBS J. 278 (15) (2011) 2702–2712.

[22] J.H. Orth, I. Fester, P. Siegert, M. Weise, U. Lanner, S. Kamitani, T. Tachibana, B.A. Wilson, A. Schlosser, Y. Horiguchi, K. Aktories, Substrate specificity of *Pasteurella multocida* toxin for α subunits of heterotrimeric G proteins, FASEB J. 27 (2) (2013) 832–842.

[23] P. Siegert, G. Schmidt, P. Papatheodorou, T. Wieland, K. Aktories, J.H. Orth, *Pasteurella multocida* toxin prevents osteoblast differentiation by transactivation of the MAP-kinase cascade via the $G\alpha_{q/11}$-p63RhoGEF-RhoA axis, PLoS Pathog. 9 (5) (2013) e1003385.

[24] M. Wu, G. Chen, Y.P. Li, TGF-β and BMP signaling in osteoblast, skeletal development, and bone formation, homeostasis and disease, Bone Res. 4 (2016) 16009.

[25] M. Whitman, Smads and early developmental signaling by the TGFβ superfamily, Genes Dev. 12 (16) (1998) 2445–2462.

[26] D.L. Glaser, F.S. Kaplan, Treatment considerations for the management of fibrodysplasia ossificans progressiva, Clinical Reviews in Bone and Mineral Metabolism 3 (3) (2005) 243–250.

[27] N. Ogata, H. Kawaguchi, U.I. Chung, S.I. Roth, G.V. Segre, Continuous activation of $G\alpha_q$ in osteoblasts results in osteopenia through impaired osteoblast differentiation, J. Biol. Chem. 282 (49) (2007) 35757–35764.

[28] H.M. Jeong, Y.H. Jin, Y.H. Choi, J. Yum, J.K. Choi, C.Y. Yeo, K.Y. Lee, PKC signaling inhibits osteogenic differentiation through the regulation of Msx2 function, Biochim. Biophys. Acta 1823 (8) (2012) 1225–1232.

[29] A. Nakura, C. Higuchi, K. Yoshida, H. Yoshikawa, PKCα suppresses osteoblastic differentiation, Bone 48 (3) (2011) 476–484.

[30] Y.J. Kim, M.H. Lee, J.M. Wozney, J.Y. Cho, H.M. Ryoo, Bone morphogenetic protein-2-induced alkaline phosphatase expression is stimulated by Dlx5 and repressed by Msx2, J. Biol. Chem. 279 (49) (2004) 50773–50780.

[31] R. Santos, O. Ursu, A. Gaulton, A.P. Bento, R.S. Donadi, C.G. Bologa, A. Karlsson, B. Al-Lazikani, A. Hersey, T.I. Oprea, J.P. Overington, A comprehensive map of molecular drug targets, Nat. Rev. Drug Discov. 16 (1) (2017) 19–34.

[32] J.H. Orth, S. Lang, M. Taniguchi, K. Aktories, *Pasteurella multocida* toxin-induced activation of RhoA is mediated via two families of G{alpha} proteins, G{alpha}q and G{alpha}12/13, J. Biol. Chem. 280 (44) (2005) 36701–36707.

[33] C. Ramakers, J.M. Ruijter, R.H. Deprez, A.F. Moorman, Assumption-free analysis of quantitative real-time polymerase chain reaction (PCR) data, Neurosci. Lett. 339 (1) (2003) 62–66.

[34] X. Rao, D. Lai, X. Huang, A new method for quantitative real-time polymerase chain reaction data analysis, J. Comput. Biol. 20 (9) (2013) 703–711.

[35] C. Busch, J. Orth, N. Djouder, K. Aktories, Biological activity of a C-terminal fragment of *Pasteurella multocida* toxin, Infect. Immun. 69 (6) (2001) 3628–3634.